SCIENCE CHINA
Information Sciences

• RESEARCH PAPER •

August 2025, Vol. 68, Iss. 8, 180504:1–180504:11
https://doi.org/10.1007/s11432-024-4185-1

Special Topic: Quantum Information

Variational quantum eigensolver with linear depth problem-inspired ansatz for solving portfolio optimization in finance

Shengbin WANG[1,2], Peng WANG[2], Guihui LI[3], Shubin ZHAO[1], Dongyi ZHAO[1], Jing WANG[1], Yuan FANG[1], Menghan DOU[1], Yongjian GU[4], Yu-Chun WU[2,5,6*] & Guo-Ping GUO[1,2,5,6*]

[1]*Origin Quantum Computing Company Limited, Hefei 230026, China*
[2]*Laboratory of Quantum Information, University of Science and Technology of China, Hefei 230026, China*
[3]*Intelligent Information Sensing and Processing Lab, College of Electronic Engineering, Ocean University of China, Qingdao 266000, China*
[4]*College of Physics and Optoelectronic Engineering, Ocean University of China, Qingdao 266100, China*
[5]*Institute of Artificial Intelligence, Hefei Comprehensive National Science Center, Hefei 230088, China*
[6]*Anhui Province Key Laboratory of Quantum Network, University of Science and Technology of China, Hefei 230026, China*

Received 18 March 2024/Revised 30 May 2024/Accepted 10 September 2024/Published online 3 July 2025

Abstract Great efforts have been dedicated in recent years to exploring practical applications for noisy intermediate-scale quantum (NISQ) computers, which is a fundamental and challenging problem in quantum computing. As one of the most promising methods, the variational quantum eigensolver (VQE) has been extensively studied. In this paper, VQE is applied to solve portfolio optimization problems in finance by designing two hardware-efficient Dicke state ansatzes that reach a maximum of $2n$ two-qubit gate depth and $\frac{n^2}{4}$ parameters, with n being the number of qubits used. Both ansatzes are partitioning-friendly, allowing for the proposal of a highly scalable quantum/classical hybrid distributed computing (HDC) scheme. Combining simultaneous sampling, problem-specific measurement error mitigation, and fragment reuse techniques, we successfully implement the HDC experiments with up to 55 qubits on our superconducting quantum computer "Wu Kong". The simulation and experimental results illustrate that the restricted expressibility of the ansatzes, induced by the small number of parameters and limited entanglement, is advantageous for solving classical optimization problems with the cost function of the conditional value-at-risk (CVaR) for the NISQ era and beyond. Furthermore, the HDC scheme shows great potential for achieving quantum advantage in the NISQ era. We hope that the heuristic idea presented in this paper can motivate fruitful investigations in current and future quantum computing paradigms.

Keywords variational quantum eigensolver, hardware-efficient Dicke state ansatz, quantum/classical hybrid distributed computing, fragment reuse technique, portfolio optimization

Citation Wang S B, Wang P, Li G H, et al. Variational quantum eigensolver with linear depth problem-inspired ansatz for solving portfolio optimization in finance. Sci China Inf Sci, 2025, 68(8): 180504, https://doi.org/10.1007/s11432-024-4185-1

1 Introduction

Quantum computing can provide astonishing speedups in certain applications, such as simulating quantum systems [1], factoring numbers [2], searching unstructured databases [3], and solving linear systems of equations [4], compared to its classical counterpart. These advantages arise from the peculiar properties of quantum entanglement, superposition, and interference. Mixed blessings, these properties also seriously impede the design and manufacture of large-scale fault-tolerant quantum computers that can fully realize the speedup potential of quantum computing [5]. Whereupon, the currently available noisy intermediate-scale quantum (NISQ) computer, with no more than hundreds of noisy qubits, short coherence time, and limited connectivity, is the only quantum platform available to us in the coming few years, and possibly even longer [6,7]. The widely held focus is on finding the "killer apps" for NISQ computers, which is a notoriously difficult problem [8,9].

* Corresponding author (email: wuyuchun@ustc.edu.cn, gpguo@ustc.edu.cn)

Variational quantum algorithms (VQAs) [10], developed for efficient implementation on both quantum and classical computers in a hybrid manner, significantly enhance the prospect of practical applications that may offer quantum advantages in the NISQ era. The prominent algorithms are the variational quantum eigensolver (VQE) [11] and the quantum approximate optimization algorithm (QAOA) [12]. In recent years, significant efforts, particularly in the fields of quantum chemistry, quantum machine learning, and combinatorial optimization [10, 13–25], have been made with VQAs to advance the practicality of NISQ computers. For combinatorial optimization, which has already been extensively applied in many areas of business and science, the studies in the quantum computing field mainly focus on maximum cut, number partitioning, and portfolio optimization, etc. [23, 24, 26–31]. Compared to QAOA, which encodes the total energy of the problem through the cost Hamiltonian that requires to be translated into a unitary operator, resulting in a much deeper quantum circuit, VQE with the unique quantum part, i.e., the ansatz, and classically optimized expectation of the total energy is more appealing. This comes from the consensus that NISQ computers are limited to executing lower-depth circuits and hence should focus on handling the classically intractable parts of the computation process as efficiently as possible.

The ansatz, a structurally parameterized quantum circuit (PQC) $U(\boldsymbol{\theta})$ with parameters $\boldsymbol{\theta}$, is the key ingredient of the VQE algorithms. The trial quantum states $|\psi(\boldsymbol{\theta})\rangle$ prepared by the ansatz are subsequently iteratively sampled and optimized to classically evaluate the minimum energy of the Hamiltonian H of the problem, i.e., $\min_{\boldsymbol{\theta}}\langle\psi(\boldsymbol{\theta})|H|\psi(\boldsymbol{\theta})\rangle$, along with the corresponding eigenstate, upon the corresponding parameters $\boldsymbol{\theta}$ [32, 33]. In other words, as the unique quantum part, ansatz determines the output fidelity of NISQ computers and the potential advantage that the VQE algorithms can achieve. Unsuitable ansatz deployed for specific problems trivially leads to bad performance. There are two main categories of ansatzes in the context of this paper: hardware-efficient (HE) ansatz and problem-inspired ansatz [10, 18]. The versatility of HE ansatz which is designed based on considering the restrictive conditions of NISQ computers can mitigate the effect of hardware noise to some extent. That is, HE ansatz is problem-agnostic and can be a circuit with very low depth, even a product state composed of one layer of single-qubit gates. These advantages have garnered much attention, resulting in a flurry of promising results on solving small-scale problems of interest [11, 13, 27], and the current combinatorial optimization investments are mainly focusing on this type of ansatz. However, for most of the underlying problems, the problem-agnostic nature of this type of ansatz may lead to undesired issues such as barren plateau (BP), local minima, and poor expressibility [34–37], particularly when the number of required qubits to span the search space becomes slightly larger. In contrast, a problem-inspired ansatz has access to some prior knowledge of the problem, which can span a more accurate search space. Hence the issues of BP and local minima can be largely alleviated [38]. Unfortunately, this type of ansatz, e.g., the extensively researched unitary coupled cluster (UCC) ansatz and heuristic ansatz in quantum chemistry [10, 39], typically results in dense entanglement among qubits and leads to much deeper circuits, which is prohibitive for the current NISQ computers to execute efficiently even on solving small-scale problems.

Clearly, viable ansatzes for efficiently solving problems of interest on NISQ computers should possess both hardware-efficient and problem-inspired properties simultaneously. That is, this type of ansatzes must be a shallow circuit with nearest-neighbor coupling which unfolds a feasible search subspace that encompasses the optimal solution (or the near-optimal solutions) while avoiding, if possible, the generation of irrelevant, even distant, states. In consequence, the key question at present turns to whether such a viable ansatz can be devised, at least for solving specific problems. Besides, another issue that arises is how to mitigate the errors induced by the width (number of qubits) of the ansatz when solving larger-scale problems.

In this paper, we address these questions by introducing two ansatzes that can efficiently prepare arbitrary Dicke states [40], which are well-suited for NISQ computers. Both ansatzes are not only useful for solving portfolio optimization problems in finance [41, 42] but also for other combinatorial optimization problems [23]. Our ansatzes are unified frameworks that span the feasible subspace and have a linear circuit depth with a constant factor of at most 2 on CNOT gates, which are applied only between adjacent qubits. The worst-case asymptotic complexity on parameters $\boldsymbol{\theta}$ is squared with a factor not exceeding $\frac{1}{4}$. The above achievements make our ansatzes the most advanced methods for preparing Dicke states that can be executed on NISQ computers with linear-nearest-neighbor coupling currently and answer the first question in the affirmative. Nevertheless, to guarantee that NISQ computers can be deployed to efficiently solve some larger-scale problems, addressing the second issue is an equally crucial task. Fortunately, the building blocks of our ansatzes construct quantum circuits using a staircase structure, similar to the structure of the Matrix product state, that is more convenient for us to embed circuit cutting [43, 44] or

qubit reuse [45] techniques, or their combination, to improve the performance of NISQ computers in terms of circuit width dimension. Further progress has been achieved by proposing a quantum/classical hybrid distributed computing (HDC) scheme. This scheme splits classically the ansatz into several subcircuits with a staircase structure first, and then partitions (cuts) each subcircuit into applicable fragments using the circuit cutting technique or executes each subcircuit directly using the qubit reuse technique. In the circuit cutting case, the total number of qubits required to be cut in each circuit is greatly reduced. The X, Y, and Z "measure-and-prepare" channels are eliminated based on the symmetry of Dicke states. Compared to the common circuit cutting technique, our scheme exponentially reduces the sampling complexity. We also significantly reduce the number of submissions of the circuits to the hardware. This preserves completely the advantage of NISQ computers in solving portfolio optimization, not only in the scenarios of selecting a small number of assets. In the qubit reuse case, the number of qubits used to execute each circuit can be reduced to merely 2. We provide detailed comparisons of our scheme to the commonly used ansatzes through complexity analysis, numerical simulations, and hardware experiments, verifying the superiority of our methods over the state-of-the-art ones.

The paper is organized as follows. In Section 2, an overview of the binary integer portfolio optimization problem is provided. The design inspiration, theoretical insights, single-layer structure rationality, detailed optimal circuit, and complexity comparisons of the proposed ansatzes are introduced in Section 3. In Section 4, we provide the numerical simulations and hardware experiments of the proposed algorithms, as well as the quantum/classical hybrid distributed computing scheme, simultaneous sampling method, problem-specific measurement error mitigation, and fragment reuse technique. Finally, we conclude our work and discuss some interesting problems in Section 5.

2 Portfolio optimization

As one of the most common optimization problems in finance, portfolio optimization involves selecting from an asset pool a set of optimally allocated assets that achieve the expected return with minimum financial risk, or maximize the expected return for a given level of risk [41,42]. In this paper, we focus on binary integer portfolio optimization based on mean-variance analysis (modern portfolio theory) because its binary variable representation aligns with the prevalent two-level quantum computers. The risk-return optimization can be modeled as

$$\begin{aligned} &\min_{\boldsymbol{x}}\ q\boldsymbol{x}^{\mathrm{T}}A\boldsymbol{x}-\boldsymbol{\mu}^{\mathrm{T}}\boldsymbol{x},\\ &\text{s.t. } \xi=\boldsymbol{\Pi}^{\mathrm{T}}\boldsymbol{x}, \end{aligned} \tag{1}$$

where $\boldsymbol{x}=(x_1,x_2,\ldots,x_n)^{\mathrm{T}}$ with $x_i\in\{0,1\}$ represents the asset selection vector, i.e., the ith asset is selected when boolean variable $x_i=1$ or not when $x_i=0$. A is the $n\times n$ real covariance matrix between assets. The risk level $q>0$ represents the investor's risk tolerance, and the vector $\boldsymbol{\mu}$ contains the expected returns of the assets. The constraint is given by $\xi=\boldsymbol{\Pi}^{\mathrm{T}}\boldsymbol{x}$, where ξ is the budget and $\boldsymbol{\Pi}$ is the asset price vector, which can be simplified to the all-ones vector, $\mathbb{1}$, in the present scenario.

There are two ways to map the problem to a quadratic unconstrained binary optimization (QUBO) form suitable for quantum computing [46]. The general way is known as the soft constraint form, which encodes the constraint to a penalty, $(\xi-\mathbb{1}^{\mathrm{T}}\boldsymbol{x})^2$, absorbed into the cost function with a penalty scaling coefficient. That is, by transforming variable $x_i\in\{0,1\}$ to $z_i\in\{-1,+1\}$ based on the relation $z_i=1-2x_i$, the binary model is converted to a spin model:

$$\min_{\boldsymbol{z}}\ q'\boldsymbol{z}^{\mathrm{T}}A\boldsymbol{z}-\boldsymbol{\mu}'^{\mathrm{T}}\boldsymbol{z}+\left\{\beta\left(\xi'+\frac{1}{2}\mathbb{1}^{\mathrm{T}}\boldsymbol{z}\right)^2\right\}_{\text{soft}}, \tag{2}$$

where β is the penalty scaling coefficient. The problem described by (2) can be easily translated into a diagonal Hamiltonian, whose ground state encodes the optimal solution of the optimization problem (1) by replacing z_i with σ_Z^i. Finally, the HE ansatz-based VQE algorithm can be applied to estimate the ground state. However, the landscape spanned by (2) with the HE ansatz is too large and flat and contains too many local minima, which impact severely the optimization of the parameters and, consequently, hinder the convergence of the solution for solving larger-scale problems.

Contrastingly, the hard constraint form encodes the constraint directly into the structure of the problem-inspired ansatz. That is, any vector $\boldsymbol{x}$ that does not conform to the constraint $\xi=\mathbb{1}^{\mathrm{T}}\boldsymbol{x}$ is

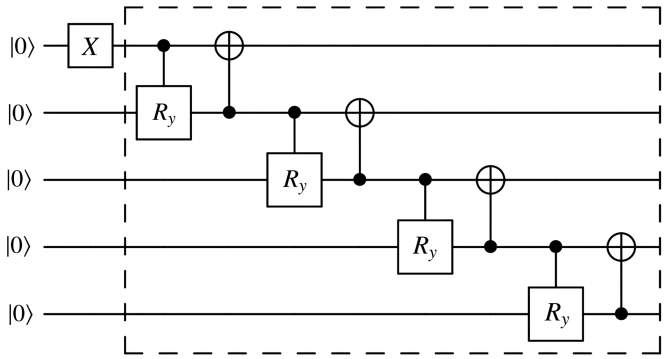

Figure 1 Illustrative staircase-structure circuit for preparing state $|W_5\rangle$.

excluded from the space spanned by the ansatz. Eq. (2) is reduced to

$$\min_{\boldsymbol{z}} \; q'\boldsymbol{z}^{\mathrm{T}}A\boldsymbol{z} - \boldsymbol{\mu}'^{\mathrm{T}}\boldsymbol{z}. \tag{3}$$

The elimination of the penalty term simplifies the evaluation of $\min_{\boldsymbol{\theta}}\langle\psi(\boldsymbol{\theta})|H|\psi(\boldsymbol{\theta})\rangle$ on a much smaller landscape.

3 Variational Dicke state ansatz

An ansatz is a dynamic quantum state preparation circuit that depends on some parameters optimized through the minimization or maximization of a problem's cost function. The form of the ansatz determines the form of the cost Hamiltonian and the training behavior of the parameters. In this section, two universal ansatzes for preparing arbitrary Dicke states $|D_k^n\rangle$ with variable amplitudes as a function of the parameters $\boldsymbol{\theta}$ are presented. In the present scenario, a Dicke state $|D_k^n\rangle$ is a superposition state composed of all n-qubit basis states $|i\rangle$ with Hamming weight $HW(i) = k$ [47,48],

$$|D_k^n\rangle = \sum_{i\in\{0,1\}^n, HW(i)=k} a_i|i\rangle, \tag{4}$$

where a_i is the amplitude of basis state $|i\rangle$. For instance, $|D_2^3\rangle$ with equal amplitude is $|D_2^3\rangle = \frac{1}{\sqrt{3}}(|011\rangle + |101\rangle + |110\rangle)$. In portfolio optimization, n denotes the number of assets that the asset pool can provide and $k \in [1, n-1]$ is the number of assets selected from the asset pool which is equivalent to the budget ξ [42]. A Dicke state encodes the constraint in (1), thus the QUBO takes the form expressed in (3). This leads to a precise search space and a more regular cost function landscape, which is beneficial for alleviating the issues of BP and local minima [38]. The applications of Dicke states also involve quantum game [49], quantum metrology [50], and quantum networks [51].

Both ansatzes are inspired by the fundamental observation that all the useful information is implicitly stored in the unitary U_n, composed of the building blocks "Controlled-R_y and CNOT" shown in the dashed box of Figure 1 for preparing W state [52]. Hence, we can easily extract the target states by preparing a linear combination of the appropriate columns of U_n, somewhat similar to the idea of the linear combination of unitaries (LCU)-based quantum state preparation algorithms [53,54]. In this paper, we refer to the circuit structure similar to the one in the dashed box as the 'staircase structure', denoted as U_n, which is the critical circuit structure of our ansatzes. We analyze the theoretical support for both ansatzes based on this observation, see Appendix A for details. For an arbitrary basis state of $|D_k^n\rangle$, there always exists a basis state with reverse symmetry to it, e.g., 11000 with 00011, 01010 with itself. Therefore, the qubit at the top can be regarded as either the lowest qubit or the highest qubit. In the following context, we fix the top qubit to be the highest qubit.

For combinatorial optimization problems, the solution is a single vector (binary string) that is fundamentally different from the ground state composed of multiple vectors for chemical systems. Therefore, the extra degrees of freedom, which should be preserved in solving certain chemistry problems, can be removed in combinatorial optimization scenarios. Then based on the observation of W state, we construct the staircase unitary U_n using the simplified "A" gates [39] which is composed of multiple "CNOT,

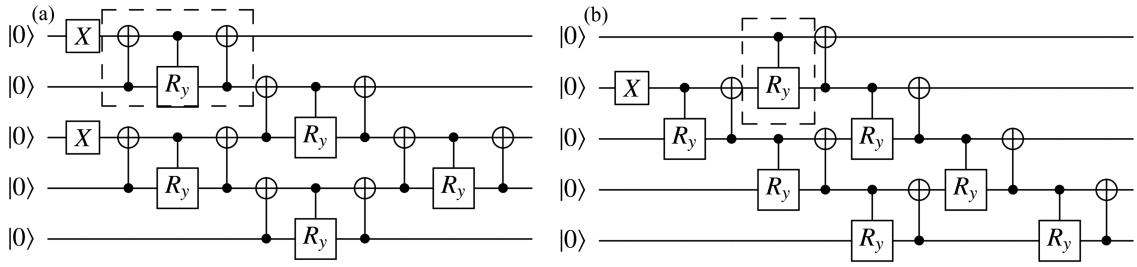

Figure 2 Illustrations of (a) CCC ansatz and (b) CC ansatz for preparing $|D_2^5\rangle$. For CCC ansatz, a 3C block is indicated in the dashed box. For CC ansatz, the inoperative controlled-R_y in the dashed box is shown for structure completeness. The variational parameters of R_y gates are omitted for brevity.

Controlled-R_y, CNOT" (3C) blocks, see Figure 2(a) for an example. Unexpectedly, the unitary contains all the information about Dicke states $|D_k^n\rangle$, which are distributed across different columns, see Appendix A for detailed analysis. Motivated by this observation, the first ansatz is constructed with k layers of staircases. Each layer is composed of $(n-k-\lfloor i/2 \rfloor)$ 3C blocks, hence is called CCC ansatz, starting with an NOT(X) gate deployed at the ith qubit where i equals $2k-1, 2k-3, \ldots, 1$, when $k \leqslant \lfloor n/2 \rfloor$, see Figure 2(a). For the cases of $k > \lfloor n/2 \rfloor$, we use the equivalence $\binom{n}{k} = \binom{n}{n-k}$ to simplify the circuit design, i.e., using the circuit for preparing $|D_{n-k}^n\rangle$ followed by the unitary $\otimes_{j=1}^n X_j$ to prepare $|D_k^n\rangle$. At last, we optimize each 3C block to its optimal circuit that contains only 2 CNOT gates to reduce the circuit depth further, see Appendix B for detailed analysis.

The second ansatz proposed here is inspired directly by the circuit for preparing W state [52], the n-qubit case of which is defined as

$$|W_n\rangle = \frac{1}{\sqrt{n}}(|100\cdots0\rangle + |010\cdots0\rangle + \cdots + |000\cdots1\rangle). \tag{5}$$

This is actually the most trivial case of selecting 1 asset out of n, $\binom{n}{1}$. The preparation procedure of W state can be represented as $|W_n\rangle = U_n(\mathrm{NOT}_1 \otimes I_{n-1})|0^n\rangle$, where $\mathrm{NOT}_1 \otimes I_{n-1}$ represents the NOT gate operating on the highest qubit in the first time step, see Figure 1, and U_n is the n-qubit unitary operator composed by the following "Controlled-R_y, CNOT" (2C) blocks, hence is called CC ansatz, shown in the dashed box. The fact we found is that W state can be regarded as being extracted from the column 2^{n-1} of the unitary U_n as $|10^{n-1}\rangle = \mathrm{NOT}_1 \otimes I_{n-1}|0^n\rangle$.

Based on generalization and summarization, CC ansatz can be alternatively constructed in three steps when $k \leqslant n/2$. The first step is to deploy unitary $X_{\{k \bmod 2\}} \otimes [(I \otimes X)^{\otimes \lfloor k/2 \rfloor}] \otimes I_{n-k}$ from top to bottom in the first time step, see Figure 2(b) for the example of preparing $|D_2^5\rangle$. The subscript $\{k \bmod 2\}$ means the first X operates only when k is odd. Then append a staircase composed of multiple 2C blocks for each X gate except the one operating on the highest qubit (if exists). Each staircase starts from the corresponding X gate and stops at the lowest qubit. At last append U_n to complete the ansatz. The number of staircase layers is reduced to $\lfloor k/2 \rfloor + 1$ for preparing $|D_k^n\rangle$, whereas the prepared state with $k \in [3, n-3]$ contains non-target basis states. Same as the method used in extending to cases with larger k in CCC ansatz, state $|D_k^n\rangle$ with $k > n/2$ in CC ansatz is prepared by $|D_{n-k}^n\rangle$. Each 2C block is also optimized to 2 CNOT gates, see Appendix B for the two compile methods provided.

Although the state prepared by CC ansatz is not a precise Dicke state $|D_k^n\rangle$ and contains non-negligible non-targets when k belongs to [3, $n-3$], the number of layers of the staircase is reduced by almost half, making it more preferable for executing on NISQ computers. We also propose a symmetric space partition scheme that utilizes the reverse symmetry property of the basis states of the Dicke state to alleviate the impact of the extra basis states and preserve the target basis states as much as possible. See Appendix G for analysis and numerical illustrations.

The two ansatzes both reach a linear complexity of two-qubit gate depth with a staircase structure, and $nk - 3k^2/2$ and $n(k+1)/2 - k^2/4$ parameters, respectively, see Appendix C for the evaluation of the complexity. The comparison with the latest schemes for preparing Dicke states is presented in Table 1. Concretely, to prepare the small scale Dicke state $|D_2^8\rangle$, the number of CNOT gates required based on the 5 methods are 44, 27, 31, 22, and 25, respectively. Our ansatzes achieve the minimum CNOT counts with linear-nearest-neighbor coupling which is more friendly for the current NISQ computers. Compared to the previous circuits, the present ansatzes are much more regular and simple. It is also worth noting

Table 1 Comparison of Dicke state preparation schemes.

Method	Depth of CNOTs	Number of CNOTs	Number of θs	Topology
Mukherjee et al. [47]	$O(nk)$	$5nk-5k^2$	–	all-to-all
Bärtschi et al. [48]	$O(k\log\frac{n}{k})$	$O(nk)$	–	all-to-all
	$O(k\sqrt{\frac{n}{k}})$	$O(nk)$	–	Grid
CCC ansatz	$2(n-k)$[a)]	$2nk-3k^2$	$nk-\frac{3k^2}{2}$	LNN[b)]
CC ansatz	$2n$	$nk-\frac{k^2}{2}$	$\frac{n(k+1)}{2}-\frac{k^2}{4}$	LNN

a) By default, $k\leqslant\frac{n}{2}$. The complexity of preparing $|D^n_{n-k}\rangle$ is equal to that of preparing $|D^n_k\rangle$.
b) Linear-nearest-neighbor connectivity.

that we can easily prepare a subspace of arbitrary $|D^n_k\rangle$ by combining fewer columns. In this manner, a much smaller and more accurate search space can be spanned when some prior knowledge of the solution is presented. Otherwise, we can still split the Dicke state into multiple subspaces and search them one by one to alleviate the issues of the BP and local minima [55, 56].

As can be seen, the ansatzes are designed by reducing the parameters and quantum gates to a minimum for improving their ability of executing on NISQ computers, while the expressibility is restricted, but the BP problem is also suppressed [37]. Intuitively for classical optimization problems in the NISQ era, the BP problem appears to be more important than expressibility. In addition, a local cost function can perform better than a global one [34, 37]. Here we use the conditional value-at-risk (CVaR) [27] as the cost function. CVaR with a small confidence level $\alpha\in(0,1]$ can be regarded as a local cost function. Additionally, the space spanned by the proposed ansatzes always contains the ground states for all cases. Therefore, the negative impacts of restricted expressibility of the proposed ansatzes can be greatly mitigated. We found numerically that deploying multiple layers of the staircase unitary U_n composed of 3C blocks, which always prepares a precise Dicke state, really does not observably improve the performance for small confidence levels, see Appendix H for the demonstrations. Therefore, in combinatorial optimization problems, it is reasonable for us to focus on the single layered U_n with CVaR, which is more amenable to the current NISQ devices.

4 Numerical simulations and experiments

In this section, we perform the numerical simulations and hardware experiments to verify the effectiveness of our proposals.

4.1 Numerical simulations

We performed extensive noise-free numerical simulations by pyQPanda [57]. Specifically, the COBYLA optimization algorithm is utilized. Simulation results show that we cannot expect to get the optimal solution in just one calculation when the problem has a little larger asset pool, especially for HE ansatz that spans an exponentially large search space, in the present shallow ansatz scenario. Therefore, it is more intuitive to statistically analyze and compare the overall performance of these ansatzes. However, the variance is a little larger due to the lower expressibility. In the following, we analyze numerically the time consumption and the probabilities of obtaining the optimal and feasible solutions for the linearly entangled HE ansatz and our proposed CCC and CC ansatzes with respect to different numbers of assets and budgets.

Figure 3 provides a sketch of the average time and probabilities of the three ansatzes with the number of assets n ranging in $[4, 20]$ and confidence level $\alpha\in\{1, 0.5, 0.25, 0.1\}$. The asset data is produced using qiskit_finance.data_providers [58]. The maximum number of iterations is set to 500. The number of budgets k is fixed at 2, and the risk level q is set to 0.5. To illustrate the statistical behaviors of the time consumption and the probabilities, we initialize the parameters $\boldsymbol{\theta}$ with a random seed 1231 and the asset pool 20 times with random seeds starting from 1000. To guarantee shallow property, viable execution time, and essential expressibility of the HE ansatz, the number of layers is set to be logarithmic in n. For consistency, the seeds used for the random initialization of the 20 asset portfolios are the same for each ansatz. To obtain results with the same precision, the number of samples of different confidence levels α should be $1/\alpha$ times of that of the cases where $\alpha=1$. That is to say, the ability of always obtaining the optimal solution in most small α instances is achieved by appropriately increasing the sampling complexity. Due to the sampling taking much longer than classical post-processing, we

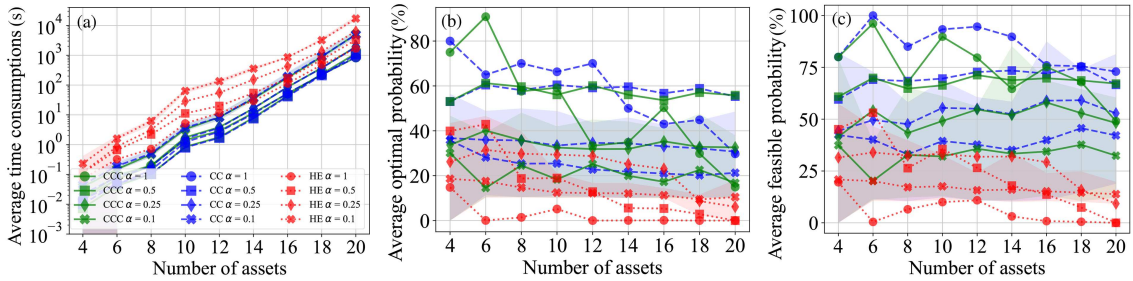

Figure 3 (Color online) Comparisons among the CCC, CC, and HE ansatzes, up to 20 assets. (a) The average time consumption; (b) the average probability of obtaining the optimal solution; (c) the average probability of obtaining the feasible solutions. A feasible solution is accepted when its expectation is not more than 0.75 times that of the optimal solution. The maximum and minimum values at $\alpha = 0.1$ are plotted as shadows. The others are not shown because they would override confusingly, disrupting the display of average information.

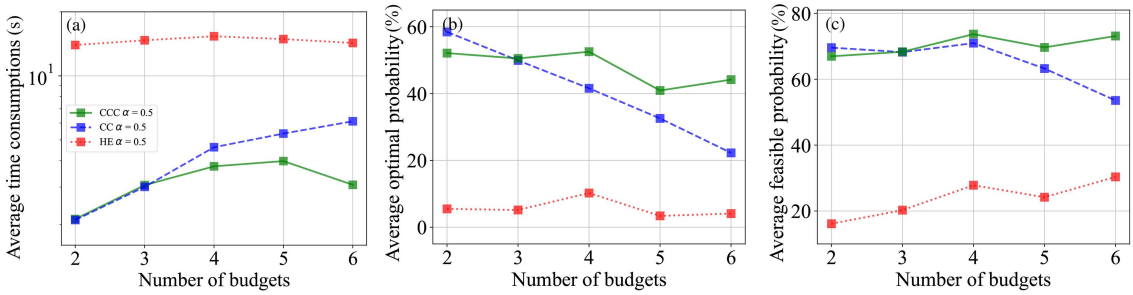

Figure 4 (Color online) Comparisons of different number of budgets. (a) The average time consumption; (b) the average probability of obtaining the optimal solution; (c) the average probability of obtaining the feasible solutions.

roughly multiplied the numerical simulation time by $1/\alpha$ to approximate the time consumption of each instance. Even so, under the same experimental conditions, the number of iterations trends to reduce with decreasing confidence level which results in only a slight difference in the consumed time for different α.

As indicated in Figure 3(a), CCC and CC ansatzes always take time less than the logarithmic depth HE ansatz. This benefits from the more targeted expressibility of our ansatzes. The Hamming weight of the basis states prepared by our ansatzes is exactly the budget k (slightly more for CC ansatz), while the HE ansatz outputs an exponential number of basis states that contain every possible budget belonging to $[0, n]$. Then the search space spanned by our ansatze is much smaller, and the landscape is much more regular, which promises the high efficiency of our ansatzes. In addition, to enhance the expressibility of the HE ansatz by deploying poly(n) layers, the time consumption would increase rapidly.

Figure 3(b) demonstrates the probabilities of obtaining the optimal solutions of the three ansatzes. As the number of assets n increases, the probabilities of obtaining the optimal solutions of CCC and CC ansatzes are generally higher than that of the HE ansatz. Their performance improves as α decreases. For example, for the HE ansatz, $\alpha = 0.5$ consistantly outperforms $\alpha = 1$, $\alpha = 0.25$ becomes superior to $\alpha = 0.5$ when $n = 8$, and $\alpha = 0.1$ surpasses $\alpha = 0.25$ starting from $n = 18$. However, for the proposed ansatzes, the upper bound is greatly improved. As shown in Figure 3(b), $\alpha = 0.5$ does not surpass $\alpha = 1$ until n reaches approximately 10. Besides, the decreases in the cases corresponding to $\alpha = 0.5, 0.25, 0.1$ are relatively slower, suggesting that the proposed ansatzes exhibit high and stable performance for larger-scale cases, even with large α. Conventionally, finding the optimal solution could be an extremely hard task that implies finding a feasible solution by consuming affordable resources is more realistic. As shown in Figure 3(c), compared to the probabilities of obtaining the optimal solution, CCC and CC ansatzes can always find feasible solutions with much higher probabilities, especially for larger n. We argue that it is more practical to find a feasible solution for optimization problems using NISQ computers because the hardware noise and sampling error lead to the rapid convergence of the algorithm to a local minimum that very likely corresponds to a feasible solution.

In the second simulation, we fix confidence level α at 0.5, the total number of assets at 12, and test the performance of these ansatzes when the budgets range from 2 to 6. As shown in Figure 4, the performance of the proposed ansatzes is always much better than the HE ansatz. In Figure 4(a), the time consumed

by the HE ansatz remains almost the same because the ansatz is the same one across different budgets, while the time consumed by the proposed ansatzes gradually increases due to the expansion of the search space. In Figure 4(b), the probability of obtaining the optimal solution of CC ansatz decreases much faster than for CCC ansatz due to the introduction of extra non-target states. Compared to the probability of obtaining the optimal solution, it is much easier for us to obtain a feasible solution, as depicted in Figure 4(c).

4.2 Experiments on NISQ computer

The common fact is that, to achieve potential quantum advantages, the problem scale needs to be large enough. That is to say, the hardware should be able to prepare a high precision superposition state containing an exponential number of basis states with respect to a large number of qubits. However, the current NISQ computers cannot easily process a large number of qubits, while retaining an exponential number of basis states simultaneously. Inspired by the partitioning-friendly property of both ansatzes, the highly scalable quantum/classical HDC scheme is proposed. Combining simultaneous sampling, problem-specific measurement error mitigation, and fragment reuse techniques, the HDC experiments of $|D_3^{55}\rangle$ and $|D_6^{12}\rangle$ using 3 and 6 qubits, respectively, achieve success.

HDC scheme. The feasibility of the HDC scheme stems from the fact that we can find a combination of a small number of columns of U_n to construct a Dicke state ansatz, refer to Appendix A. Therefore, the ansatz can be classically split into several subcircuits, each of which is synthesized using only one of these columns, or a superposition of a few of these columns, if possible, followed by U_n. Each subcircuit with relatively sparse entanglement spans a smaller subspace that is more applicable for NISQ computers. By careful design, the sparse staircase structure of the subcircuits offers us superior properties like a minimal number of cut qubits and a correspondingly minimal number of observables of the "measure-and-prepare" channels for utilizing the circuit cutting technique, refer to Appendix D for the detailed analysis. Specifically, the total number of cut qubits for partitioning each subcircuit into $p+1$ fragments is just p and the "measure-and-prepare" channel only has the observables $|0\rangle\langle 0|$ and $|1\rangle\langle 1|$, when a single qubit is cut between the adjacent two fragments. Then the sampling complexity of each subcircuit for evaluating the CVaR is $O(1/(\alpha\epsilon^2))$ with the confidence level $\alpha \in (0, 1]$ and the accuracy ϵ. This is a complexity that has no concern with the total number of cut qubits p. Hence, the subcircuits can be cut into smaller fragments to more easily obtain the low-probability basis states. This is because the basis states in a smaller fragment can be obtained with higher probabilities, leading to more accurate results. Furthermore, the qubit reuse technique [45] can be applied to execute these subcircuits directly, especially those with very few columns, refer to Figure E3 in Appendix E for an illustration. However, the circuit cutting technique can mitigate the impact of errors more flexibly in the width dimension of NISQ devices [43, 59].

Simultaneous sampling. The reduction of the "measure and prepare" channels eliminates the redundant sampling complexity. The number of fragment submissions to the quantum computer is also exponentially decreased to $2p+1$ where p is the number of cut qubits. However, the observables $|0\rangle\langle 0|$ and $|1\rangle\langle 1|$ can only be observed on matrix basis I, which results in the sequential sampling of the fragments, refer to the end of Appendix D. Here we propose to simultaneously sample each fragment, which is also advantageous for applying quantum error mitigation (QEM) [60–63]. In this case, all the $2p + 1$ fragments are shot N times each. Then we perform sequential sampling of the measured results in a classical manner.

Problem-specific measurement error mitigation. In general, the states prepared by problem-inspired ansatzes are sparse ones, so the commonly laudable noise-resistance feature is no longer as effective. Here, by combining the symmetry property of each fragment with measurement error mitigation method [60, 62], we greatly improve the accuracy of the execution on NISQ hardwares. Specifically, we found that each fragment can only output states with the same Hamming weight, which provides us with a more accurate assignment matrix M by setting the columns with other Hamming weights to be a standard basis with the element "1" on the main diagonal. Then after evaluating $\boldsymbol{p}_{\text{migit}} = M^{-1}\boldsymbol{p}_{\text{noisy}}$ where $\boldsymbol{p}_{\text{noisy}}$ is the vector of the measured probability and $\boldsymbol{p}_{\text{migit}}$ is the mitigated probability, we normalize the probabilities of the states with the correct Hamming weight in $\boldsymbol{p}_{\text{migit}}$ to be the final output. Our proposals mitigate the effects of noise perturbation and, as a result, improve the stability and convergence speed of the optimization process.

Fragment reuse. In the optimization process, the change of each θ only influences the corresponding

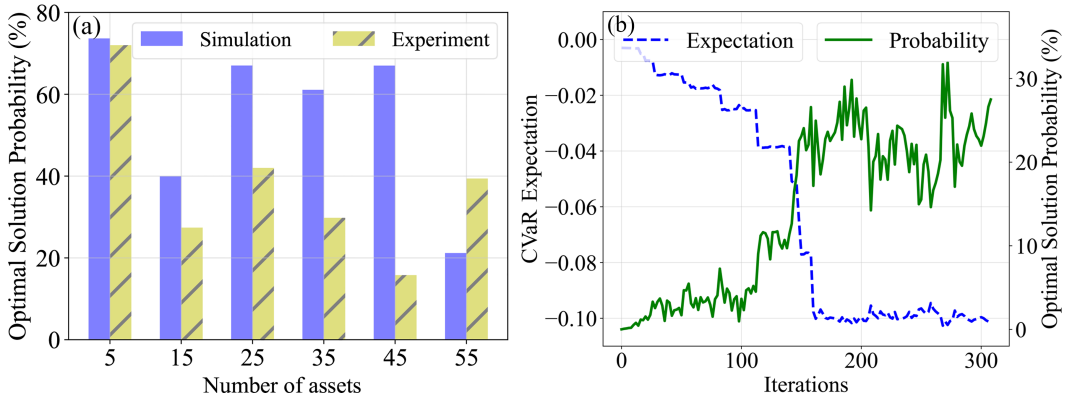

Figure 5 (Color online) (a) Probability of obtaining the optimal solution in the first experiments, numerical versus hardware. Appendix F shows the simulation and experiment setups, and qubit topology for both experiments. In this experiment, qubits 45, 46, 52 are used. It should be clarified that we did not perform experiments with qubits larger than 55. (b) The convergence curve for case $|D_6^{12}\rangle$. The blue dashed line shows the change of the CVaR expectation, and the green solid line represents the probability of obtaining the optimal solution.

fragment, and the other fragments remain unchanged. Consequently, it is not necessary to repeatedly execute all of the fragments. The previously measured results of the fragments can be reused later when their θs have not changed. This fact is used to reduce the number of submissions to the quantum computer and the introduced bias can improve the stability of the optimization process. Hence the trainability can be improved as well.

Now, we present the experimental results. The first experiment executes the $k = 3$ case of CCC ansatz with one column corresponding to one subcircuit on the NISQ computer to demonstrate the feasibility of the proposed algorithms; CC ansatz has similar results. Each $|D_3^n\rangle$ ansatz is classically split into $\lfloor \frac{n-1}{2} \rfloor$ subcircuits. Each subcircuit is partitioned into $\lceil \frac{n-1}{2} \rceil$ 3-qubit fragments. For the specific HDC scheme and complexity analysis, refer to Appendixes E and F. The asset pool is generated using random seed 1000. To improve the convergence speed, the confidence level α is initially set to a small value, as shown in Table F1 of Appendix F, and is then increased to 1.0 gradually [64]. We also formalize the uniform initialization of the states for all subcircuits.

In this scenario, SLSQP is employed, rather than COBYLA, because this experiment needs to handle many small-size fragments, and SLSQP can take better advantage of the fragment reuse technique to improve the stability of the optimization process (cost gradient). In addition, there are only 3 "1" elements in each basis state, and their distribution is relatively dispersed. The gradient of the cost function is easier to find. The experiments achieve the successful executions of the circuits with up to 55 qubits. In fact we found that hardware experiments converge much faster than numerical simulations under the same configuration in the early stage of the optimization process. This indicates that the perturbation of the hardware noise is an inherent advantage for the CVaR cost function with a small α. However, the discrepancy between the probabilities of obtaining the optimal solutions in both cases becomes larger with respect to the number of assets, see Figure 5(a). This result stems from the fact that, as the value of α increases in the optimization process, the number of basis states that could be sampled in the confidence interval $(0, \alpha]$ becomes larger. The sampling accuracy is reduced due to the instability and noise of the hardware. Hence the stability of the CVaR expectation gradually decreases in the subsequent stages of the optimization process. The instability of the expectation disturbs the convergence process, leading to fluctuations in the probability of obtaining the optimal solution. This instability also provides the opportunity to surpass noiseless numerical simulations (as seen in the 55-asset experiment).

The second experiment searches for the optimal solution of case $|D_6^{12}\rangle$. The ansatz is classically split into 5 subcircuits. Each subcircuit is cut into two 6-qubit fragments and one 2-qubit 3C block. For the specific HDC scheme and complexity analysis, refer to Appendixes E and F. At this time, the restricted expressibility and complex structure of our ansatz severely impede its uniform initialization. To remedy this issue, we coarsely fit the parameters $\boldsymbol{\theta}$ that can produce a relatively uniform output. The coarse fitting is performed by minimizing $\sum_i (p_i' - p_0)^2$ where p_i' corresponds to the probabilities of the sampled states and p_0 is the uniform probability. Additionally the parameters $\boldsymbol{\theta}$ are also initialized randomly in the interval $[\pi/2, 3\pi/4]$.

Extensive numerical simulations showed that, in the most complicated scenario, COBYLA outperforms

SLSQP. As shown in Figure 4(b), when using COBYLA and setting α to 0.5, the average probability of obtaining the optimal solution of $|D_6^{12}\rangle$ is about 45% (approaching the soft cap of 50% corresponding to $\alpha = 0.5$), while with the same configuration, SLSQP can only achieve 18%. This results from the local minima problems caused by the considerable overlap of the basis states. Specifically, the asset pool generated by the random seed 1000 also prevents SLSQP from converging to the optimal solution. The present experimental scheme can only slightly improve the situation. In such a difficult instance, we attempted to use COBYLA. In the primary stage of COBYLA, only one or two parameters are changed in each iteration. So, we choose to repeatedly run the primary stage multiple times. The parameters obtained from the previous run are used as the initial parameters of the next run. In consequence, the fragment reuse technique can make the optimization process more stable. As shown in Figure 5(b), the optimization process exhibits fluctuating convergence to the optimal solution. The COBYLA optimization algorithm and the learning rate adjustment made at the beginning of each run inherently lead to fluctuations. Additionally, larger values of α exacerbate the impact of the instability and noise of the hardware to the optimization process.

5 Conclusion and discussion

In this paper, we have achieved the common portfolio optimizations using our superconducting computer "Wu Kong" for up to 55 qubits (assets) in the case of $|D_3^n\rangle$ and 12 qubits in the case of $|D_{n/2}^n\rangle$. This comes from trading expressibility for trainability by proposing two compact Dicke state ansatzes and utilizing the CVaR cost function. Additionally, the proposed HDC scheme with simultaneous sampling, problem-specific measurement error mitigation, and fragment reuse technique, is utilized. The proposed ansatzes achieve the current lowest complexity in terms of circuit depth, two-qubit gates, and parameters, compared to previous methods. The unified framework for preparing arbitrary Dicke states with a staircase structure is well-suited for distributed quantum computing. Our proposals greatly improve the execution precision in NISQ devices with little overhead.

It should be noted that we just applied the simplest quantum error mitigation method, i.e., quantum measurement error mitigation. Other superior methods, such as zero-noise extrapolation and probabilistic error cancellation [60], should be able to achieve significantly better results. Hence, as the performance of NISQ computers improves, the methods we proposed have the potential to significantly accelerate certain practical applications of variational quantum algorithms [10], such as in the fields of chemistry, biology, and machine learning, in the near future, not limited to classical optimization problems.

The experimental results show that partitioning the search space into multiple small-enough subspaces can alleviate the barren plateau problem. Nevertheless, to obtain potential quantum advantages, ergodically searching these subspaces may not be efficient in some cases. Additionally, the error-prone issue of NISQ computers limits their capability further. In consequence, choosing the appropriate columns or partial elements of these columns by consuming few resources to span a more accurate search subspace becomes critical. However, it may be cumbersome due to its dependence on the correlation among the assets and subspaces.

Acknowledgements This work was supported by National Natural Science Foundation of China (Grant No. 12034018).

Supporting information Appendixes A–H. The supporting information is available online at info.scichina.com and link.springer.com. The supporting materials are published as submitted, without typesetting or editing. The responsibility for scientific accuracy and content remains entirely with the authors.

References

1 Feynman R P. Simulating physics with computers. Int J Theor Phys, 1982, 21: 467–488
2 Shor P W. Algorithms for quantum computation: discrete logarithms and factoring. In: Proceedings of the 35th Annual Symposium on Foundations of Computer Science, 1994. 124–134
3 Grover L K. Quantum mechanics helps in searching for a needle in a haystack. Phys Rev Lett, 1997, 79: 325–328
4 Harrow A W, Hassidim A, Lloyd S. Quantum algorithm for linear systems of equations. Phys Rev Lett, 2009, 103: 150502
5 Nielsen M A, Chuang I L. Quantum Computation and Quantum Information (10th Anniversary edition). Cambridge: Cambridge University Press, 2010
6 Preskill J. Quantum computing in the NISQ era and beyond. Quantum, 2018, 2: 79
7 Leymann F, Barzen J. The bitter truth about gate-based quantum algorithms in the NISQ era. Quantum Sci Technol, 2020, 5: 044007
8 Bharti K, Cervera-Lierta A, Kyaw T H, et al. Noisy intermediate-scale quantum algorithms. Rev Mod Phys, 2022, 94: 015004
9 Lau J W Z, Lim K H, Shrotriya H, et al. NISQ computing: where are we and where do we go? AAPPS Bull, 2022, 32: 27
10 Cerezo M, Arrasmith A, Babbush R, et al. Variational quantum algorithms. Nat Rev Phys, 2021, 3: 625–644
11 Peruzzo A, McClean J, Shadbolt P, et al. A variational eigenvalue solver on a photonic quantum processor. Nat Commun, 2014, 5: 4213
12 Farhi E, Goldstone J, Gutmann S. A quantum approximate optimization algorithm. 2014. ArXiv:1411.4028

13 Kandala A, Mezzacapo A, Temme K, et al. Hardware-efficient variational quantum eigensolver for small molecules and quantum magnets. Nature, 2017, 549: 242–246
14 Moll N, Barkoutsos P, Bishop L S, et al. Quantum optimization using variational algorithms on near-term quantum devices. Quantum Sci Technol, 2018, 3: 030503
15 McArdle S, Endo S, Aspuru-Guzik A, et al. Quantum computational chemistry. Rev Mod Phys, 2020, 92: 015003
16 Tilly J, Chen H, Cao S, et al. The variational quantum eigensolver: a review of methods and best practices. Phys Rep, 2022, 986: 1–128
17 O'Brien T E, Streif M, Rubin N C, et al. Efficient quantum computation of molecular forces and other energy gradients. Phys Rev Res, 2022, 4: 043210
18 Fedorov D A, Peng B, Govind N, et al. VQE method: a short survey and recent developments. Mater Theor, 2022, 6: 2
19 Biamonte J, Wittek P, Pancotti N, et al. Quantum machine learning. Nature, 2017, 549: 195–202
20 Cong I, Choi S, Lukin M D. Quantum convolutional neural networks. Nat Phys, 2019, 15: 1273–1278
21 Li G, Zhao X, Wang X. Quantum self-attention neural networks for text classification. 2022. ArXiv:2205.05625
22 Lamata L. Quantum machine learning implementations: proposals and experiments. Adv Quantum Tech, 2023, 6: 2300059
23 Nannicini G. Performance of hybrid quantum-classical variational heuristics for combinatorial optimization. Phys Rev E, 2019, 99: 013304
24 Liu X, Angone A, Shaydulin R, et al. Layer VQE: a variational approach for combinatorial optimization on noisy quantum computers. IEEE Trans Quantum Eng, 2022, 3: 1–20
25 Palackal L, Poggel B, Wulff M, et al. Quantum-assisted solution paths for the capacitated vehicle routing problem. 2023. ArXiv:2304.09629
26 Wang Z, Hadfield S, Jiang Z, et al. Quantum approximate optimization algorithm for MaxCut: a fermionic view. Phys Rev A, 2018, 97: 022304
27 Barkoutsos P K, Nannicini G, Robert A, et al. Improving variational quantum optimization using CVaR. Quantum, 2020, 4: 256
28 Yu Y, Cao C, Dewey C, et al. Quantum approximate optimization algorithm with adaptive bias fields. Phys Rev Res, 2022, 4: 023249
29 Amaro D, Modica C, Rosenkranz M, et al. Filtering variational quantum algorithms for combinatorial optimization. Quantum Sci Technol, 2022, 7: 015021
30 Zhu L, Tang H L, Barron G S, et al. Adaptive quantum approximate optimization algorithm for solving combinatorial problems on a quantum computer. Phys Rev Res, 2022, 4: 033029
31 Qu D, Matwiejew E, Wang K, et al. Experimental implementation of quantum-walk-based portfolio optimization. Quantum Sci Technol, 2024, 9: 025014
32 Benedetti M, Lloyd E, Sack S, et al. Parameterized quantum circuits as machine learning models. Quantum Sci Technol, 2019, 4: 043001
33 Herasymenko Y, O'Brien T E. A diagrammatic approach to variational quantum ansatz construction. Quantum, 2021, 5: 596
34 Cerezo M, Sone A, Volkoff T, et al. Cost function dependent barren plateaus in shallow parametrized quantum circuits. Nat Commun, 2021, 12: 1791
35 Marrero C O, Kieferová M, Wiebe N. Entanglement-induced barren plateaus. PRX Quantum, 2021, 2: 040316
36 Leone L, Oliviero S F E, Cincio L, et al. On the practical usefulness of the hardware efficient ansatz. 2022. ArXiv:2211.01477
37 Holmes Z, Sharma K, Cerezo M, et al. Connecting ansatz expressibility to gradient magnitudes and barren plateaus. PRX Quantum, 2022, 3: 010313
38 Bharti K, Haug T. Iterative quantum-assisted eigensolver. Phys Rev A, 2021, 104: L050401
39 Gard B T, Zhu L, Barron G S, et al. Efficient symmetry-preserving state preparation circuits for the variational quantum eigensolver algorithm. npj Quantum Inf, 2020, 6: 10
40 Dicke R H. Coherence in spontaneous radiation processes. Phys Rev, 1954, 93: 99–110
41 Orús R, Mugel S, Lizaso E. Quantum computing for finance: overview and prospects. Rev Phys, 2019, 4: 100028
42 Herman D, Googin C, Liu X, et al. A survey of quantum computing for finance. 2022. ArXiv:2201.02773
43 Peng T, Harrow A W, Ozols M, et al. Simulating large quantum circuits on a small quantum computer. Phys Rev Lett, 2020, 125: 150504
44 Ying C, Cheng B, Zhao Y, et al. Experimental simulation of larger quantum circuits with fewer superconducting qubits. Phys Rev Lett, 2023, 130: 110601
45 Hua F, Jin Y, Chen Y, et al. Exploiting qubit reuse through mid-circuit measurement and reset. 2022. ArXiv:2211.01925
46 Hodson M, Ruck B, Ong H, et al. Portfolio rebalancing experiments using the quantum alternating operator ansatz. 2019. ArXiv:1911.05296
47 Mukherjee C S, Maitra S, Gaurav V, et al. Preparing dicke states on a quantum computer. IEEE Trans Quantum Eng, 2020, 1: 1–17
48 Bärtschi A, Eidenbenz S. Short-depth circuits for dicke state preparation. In: Proceedings of IEEE International Conference on Quantum Computing and Engineering, 2022. 87–96
49 Özdemir S K, Shimamura J, Imoto N. A necessary and sufficient condition to play games in quantum mechanical settings. New J Phys, 2007, 9: 43
50 Pezzè L, Smerzi A, Oberthaler M K, et al. Quantum metrology with nonclassical states of atomic ensembles. Rev Mod Phys, 2018, 90: 035005
51 Miguel-Ramiro J, Dür W. Delocalized information in quantum networks. New J Phys, 2020, 22: 043011
52 Cruz D, Fournier R, Gremion F, et al. Efficient quantum algorithms for GHZ and W states, and implementation on the IBM quantum computer. Adv Quantum Tech, 2019, 2: 1900015
53 Long G L. General quantum interference principle and duality computer. Commun Theor Phys, 2006, 45: 825–844
54 Wang S, Wang Z, Cui G, et al. Fast black-box quantum state preparation based on linear combination of unitaries. Quantum Inf Process, 2021, 20: 270
55 Bittel L, Kliesch M. Training variational quantum algorithms is NP-hard. Phys Rev Lett, 2021, 127: 120502
56 Tüysüz C, Clemente G, Crippa A, et al. Classical splitting of parametrized quantum circuits. 2022. ArXiv:2206.09641
57 Dou M, Zou T, Fang Y, et al. QPanda: high-performance quantum computing framework for multiple application scenarios. 2022. ArXiv:2212.14201
58 Javadi-Abhari A, Treinish M, Krsulich K, et al. Quantum computing with Qiskit. 2024. ArXiv:2405.08810
59 Wang S, Fontana E, Cerezo M, et al. Noise-induced barren plateaus in variational quantum algorithms. Nat Commun, 2021, 12: 6961
60 Cai Z, Babbush R, Benjamin S C, et al. Quantum error mitigation. 2022. ArXiv:2210.00921
61 Bonet-Monroig X, Sagastizabal R, Singh M, et al. Low-cost error mitigation by symmetry verification. Phys Rev A, 2018, 98: 062339
62 Nation P D, Kang H, Sundaresan N, et al. Scalable mitigation of measurement errors on quantum computers. PRX Quantum, 2021, 2: 040326
63 Temme K, Bravyi S, Gambetta J M. Error mitigation for short-depth quantum circuits. Phys Rev Lett, 2017, 119: 180509
64 Kolotouros I, Wallden P. Evolving objective function for improved variational quantum optimization. Phys Rev Res, 2022, 4: 023225